Induction Machine Based Flywheel Energy Storage (FES) System Fed From a 20 kHz AC Link

Irfan Alan, Member IEEE
Ege University
Bornova, Izmir, 35100, TURKEY
Email: irfanalan@ieee.org

Thomas A. Lipo, Fellow IEEE
University of Wisconsin
Madison WI 53706, USA
Email: lipo@ece.wisc.edu

Abstract **- This study introduces a field oriented controlled (FOC) induction machine based flywheel energy storage (FES) system fed from a 20kHz ac link and Pulse Density Modulated (PDM) Converter. The feasibilty of FES system is investigated both in software and hardware and is demonstrated succesfully in both cases. The investigated system offers a good potential as a temporary energy storage system for various applications from automobile industry to aerospace applications.**

I. INTRODUCTION

Despite extensive research efforts on new batteries over the past two decades, available batteries are limited in their usefulness as a temporary energy storage device. Research experts have recognized that the flywheel offers important advantages for reducing peak power demands together with a longer service life. The need for a cost effective, long life cycle, small size and high power density energy storage systems has made the temporary FES systems a viable solution to the problem. Power quality surveys have shown that the majority of voltage sags and momentary interruptions last less than 3 seconds, therefore the energy storage systems are required to effectively provide a short burst of power [1]. Advantages offered by this emerging technology in aerospace applications are described and the current NASA approach toward developing the technology is presented [2,3]. The FES System is intended to be utilized in a low-earth orbit sattelite applications and flight test demonstration of the international space station to overcome the limitations presented by the batteries [4-8]. For space vehicles, two counter-rotating wheels are used to produce a FES system [9]. For achieving matched flow conditions in a natural gas processing plant, it is shown that the torque disturbance rejection in a robust speed controller for a compressor driven field oriented controlled induction motor can best be handled by the incorporation of a massive flywheel [10]. The possibilty of application of FES system for flywheel traction electric transfer of wheeled transport facilities was investigated in [11]. The peak energy requirements of an electric vehicle during both acceleration and regenrative braking was met by a secondary energy storage unit (SESU) [12]. A FES device was introduced as capable of enhancing the fuel economy of a hybrid type road vehicle [13]. Variable speed flywheel generators have also been considered for the stabilization of electric power system transients and faults [14-18].

This study introduces a field oriented controlled (FOC) induction machine based FES system fed from a 20kHz High Frequency (HF) ac link and Pulse Density Modulated (PDM) Converter.

The 20kHz HF ac link and PDM technology provides convenient means for power management in a multi-terminal converter distribution system and offers flexibility in voltage level changes, enjoying fast system response and freedom from acoustic noise. Such a HF ac link distribution system is especially attractive for isolation and power density sensitive applications. The double bridge ac link system introduced [19-23] permits the induction machine to operate at variable frequency with full bidirectional power flow in either rotational direction.

One important application of this ac link and PDM converter technology is in situations where the characteristics of the power source are constrained such that the power must be managed so as to maintain the flow of power to the link constant. In most cases, however, the loads on the link are variable such that the power demand and supply can not be matched without additional load/sources. Since the power difference must be absorbed within the ac link, large fluctuations can be produced on the link causing, perhaps, failure of the transistors in the power converter due to an overvoltage condition. In such situations an additional load/source can be conveniently implemented by means of a FES system connected to the link via a power converter and variable frequency induction machine as shown in Fig. 1.

The flywheel is controlled to operate as a load leveling device through the control of the FOC induction machine. Hence, only the average load now need be supplied by the battery source while the variations in power demand from the motor can be absorbed by the flywheel/motor by either speeding up or decelerating the flywheel.

In the work achieved, the existing HF link and double bridge is used to study the effectiveness of the FES system. In particular, the study demonstrates, in hardware as well as in software, the feasibility of maintaining relatively constant ac resonant link voltage amplitude by rapidly extracting or absorbing excess link power from/to an induction machine connected to the link. A detailed evaluation of the control requirements for such a control strategy is developed and implemented in hardware.

One of the important contribution of this work is the demonstration of application of 20kHz ac link and PDM converter technology to FES systems. Especially aerospace applications may very well enjoy the advantages provided by the technology.

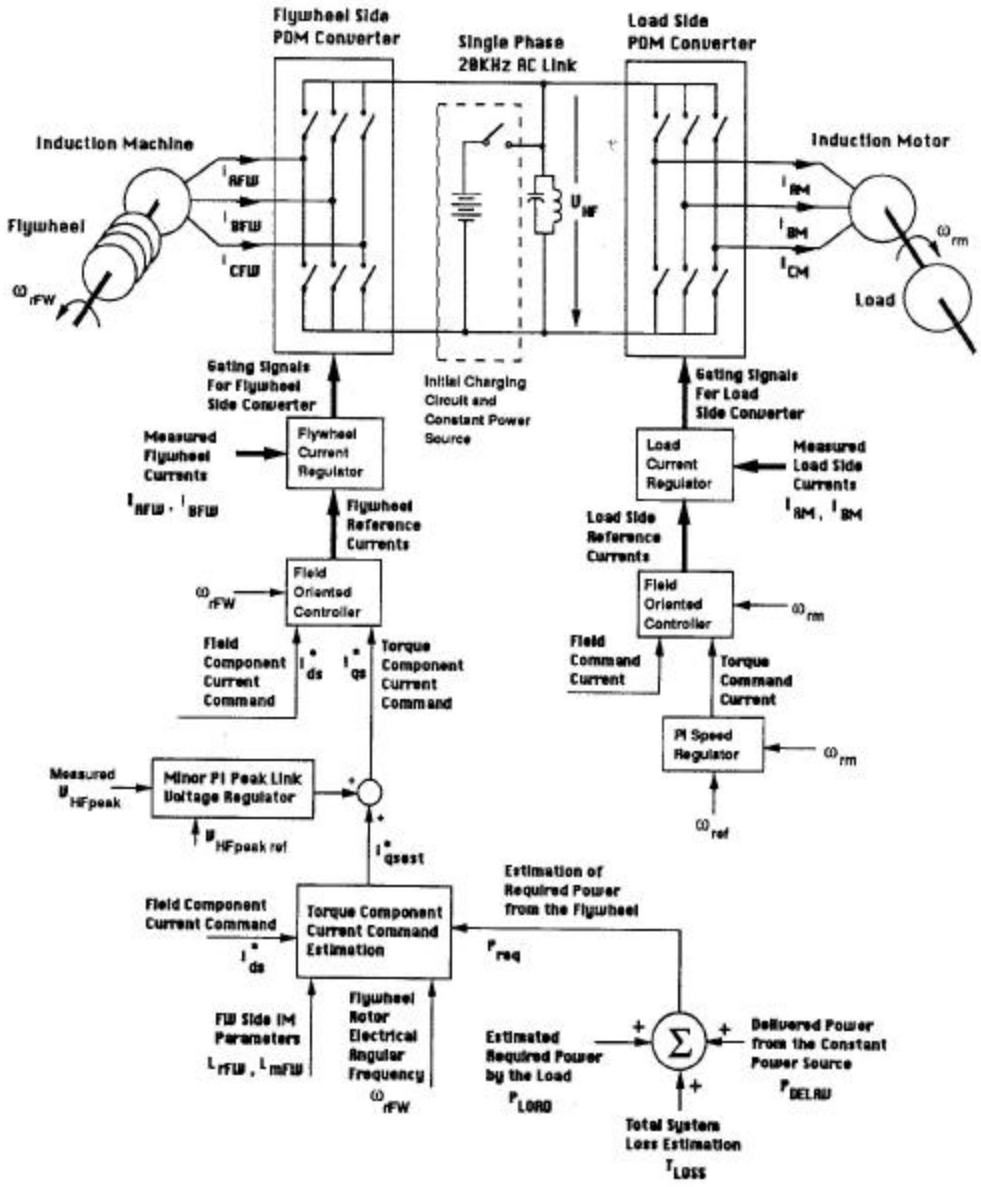

Fig. 1. Power and Control Block Diagram of the Software Simulated Flywheel Energy Storage and Load Leveling System

II. BACKROUND

Some background on the Field Oriented Controlled (FOC) Induction Machine and Pulse Density Modulation (PDM) Concept is seen appropriate considering the scope of the publication.

There is a close parallel between the physical torque control principles in a dc machine and a field oriented controlled induction machine. Due to the commutator action in a dc machine, the field flux and the armature mmf (magneto motive force) are maintained in a mutually perpendicular orientation independent of the rotor speed. As a result of this orthogonality the filed flux is unaffacted by the armature current, and an electromagnetic torque proportional to the armature current is generated. The generated torque in a dc machine is given by Eq. 1.

$$T_e = K\Phi_f I_a \qquad (1)$$

Here, K is a torque constant, $\varnothing_f$ is field flux, and I_a is the armature current. If the orthogonality between the flux and the armature mmf were disturbed (by shifting the brush positions intentionally for exmaple), the field flux would no longer be independent of the armature current and the torque equation should be modified to include an angle dependent function.

The torque expression for the induction machine based on the classical per phase equivalent circuit shown in Fig. 2 is given in Eq. 2.

$$T_e = q\frac{P}{2}\frac{r_r}{s}\frac{I_r^2}{w_e} = q\frac{P}{2}\frac{E_r I_r}{w_e} \quad (2)$$

where q is the number of phases, P is the number of poles, r_r is the stator referred rotor resistance, I_r is the stator referred rotor current, s is the slip, ω_e is the electrical angular supply frequency, and E_r is the stator referred rotor induced voltage.

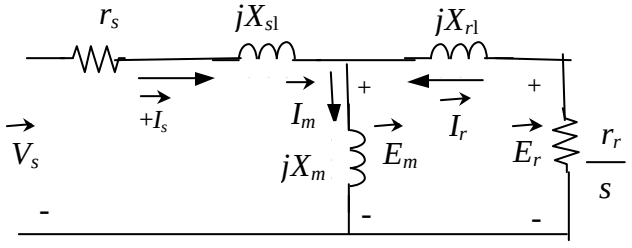

Fig. 2. Classical Per Phase Equivalent Circuit of an Induction Machine.

By the utilization of an equivalent circuit model for the induction machine proper for the field orientation control as shown in Fig. 3 a similar torque and flux control can be achieved for a field oriented controlled induction machine. Line current of the induction machine is seperated into two components, namely the flux and the torque component currents, which are kept orthogonal to each other by the proper slip frequency selection so that a similar torque control is obtained as in the dc machine case. When this is

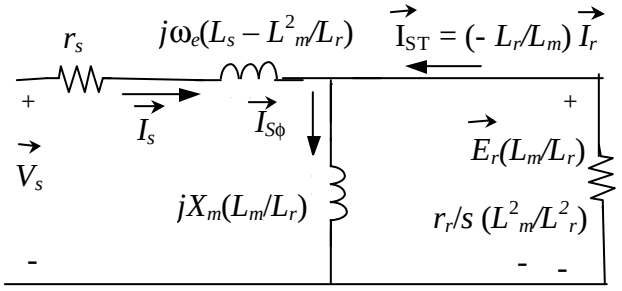

Fig. 3. Per Phase Equivalent Circuit of a Field Oriented Controlled (FOC) Induction Machine.

achieved the generated torque in a field oriented controlled induction machine can be described by Eq. 3.

$$T_e = q\frac{P}{2}\frac{L^2_m}{L_r} I_{S\Phi} I_{ST} \quad (3)$$

Here, L_m is the magnetazing inductance, L_r is the stator referred rotor self indcutance, $I_{S\emptyset}$ is the flux component current, and the I_{ST} is the torque component current of the induction machine considered.

In a field oriented controlled machine the flux component current in terms of classical equivalent circuit quantities is represented as given in Eq. 4.

$$I_{S\Phi} = -\frac{E_r}{jw_e L_m} \quad (4)$$

Similarly, the torque component current in terms of classical equivalent circuit quantities is represented as given in Eq. 5.

$$I_{ST} = -\frac{L_r}{L_m} I_r \quad (5)$$

The slip frequency in a field oriented controlled machine is given by Eq. 6.

$$sw_e = -\frac{r_r}{L_r}\frac{I_{ST}}{I_{S\Phi}} \quad (6)$$

The line current in a field oriented controlled machine is given by Eq. 7.

$$I_s = \sqrt{I^2_{S\Phi} + I^2_{ST}} \quad (7)$$

For further information on FOC Induction Machine one is referred to References [24, 25].

The pulse Density Modulation (PDM) concept mentioned in this article is often used with high frequency (HF) resonant power converters. The dc or low frequency ac voltage or current quantities are synthesized from the half cycles of resonating voltage or current links so that both the reference and the synthesized actual quantities are matched and they have the same volt-second area. In essence pieces of resonating high frequency link voltages/currents are selected in such a polarity and density that the dc or low frequency ac reference and the synthesized voltage or current waveforms cover the same average volt-second or current-second area within their specific time intervals or periods. Principles of this Area Comparison Pulse Density Modulation concept is given in detail in Ref. [26-27]. Several crucial advantages of PDM technology over the PWM can be identified as mentioned in the 3rd paragraph of Section I.

III. SOFTWARE SIMULATION OF THE SYSTEM

A power and control block diagram of the system which has been simulated in software is shown in Figure 1. The system studied in software comprises three complete converter bridges for various interfaces to the 20kHz ac link, one for the initial charging circuit and constant power source interface, one for the induction motor load interface, and one for the flywheel induction machine interface. However, the system investigated in hardware has only two available converter bridges requiring therefore certain arrangements as will be mentioned in the experimental realization section.

Operation of the load machine in four different quadrants from the link via its associated 3Ø-PDM converter means varying power demands from the system. Since the source is a constant power source during the flywheel mode of operation, the power balance in the ac link should be levelled by the

flywheel. In other words, when extra power is pumped into the link, the flywheel should absorb the extra power and when the load and losses demand more power than the constant power source can deliver, the flywheel should deliver the difference to maintain a proper link voltage in the link. As a result the power difference between the constant power source and varying demands of the load and losses is levelled out by the flywheel on an average basis. The software simulation of this type of operation is presented in this section.

The constant power source is represented only by the amount of constant power it delivers to the high frequency ac link without simulating any type of dc or ac source and associated converters. In the simulations different constant power levels such as of 2.5, 3.0 and 3.5kW are used. The nameplate ratings and per phase equivalent circuit parameters of the induction machine operated as a flywheel is given in Appendix-1. Similar ratings and parameters for the induction machine used as load is given in Appendix-2. Both of these machines are assumed to be indirect FOC via current regulated PDM converters.

III.A. Overall Operating Principle of the System

The induction machine used as flywheel, shown in Fig. 1, must be excited and operated at some sufficient speed before it can be used as a load leveling device. Therefore, an initial charging circuit and an associated converter is used to establish the peak link voltage, to excite and bring the machine to a predetermined sufficient speed. Once the speed and excitation requirement is met for the flywheel, the flywheel mode of operation is started and the initial charging circuit is switched to operate as a constant power source during the new mode of operation.

The control of the average active power balance in the link requires a good estimation of the torque component current command for the flywheel machine to level the load variations, to meet the varying demand of operating losses and maintain a proper link voltage in the link. Since power matching on an instantaneous basis is not possible, an average power matching technique which makes use of power estimation for both induction machines is used. The converter and resonant tank circuit losses have also been incorporated into the estimation procedure. The difference between the instantaneous power and average power is left to the energy storage capacity of the resonant tank circuit and a proportional-integral (PI) peak link voltage regulator.

III.B. Torque Component Current Command Estimation

Initially, the average active power required from the flywheel is estimated by a simple summation of incoming and outgoing average active powers to and from the link. A positive sign convention for the losses and outgoing power, and a negative sign convention for the incoming power is used for this purpose.

Once the total average active power required from the flywheel is determined, the torque component current command of the flywheel machine is estimated by means of equations 8 through 10 to meet the required power demand. Here, the speed of the machine is measured, the flux component current command and the per phase equivalent circuit parameters of the flywheel machine are known in advance.

$$P_{req} = T_e w_r \tag{8}$$

For a three phase and two poles induction machine the torque expression in Eq. 3 becomes as follows.

$$T_e = 3\frac{1}{2}\frac{L^2{}_m}{L_r} i_{ds}^{e*ss} i_{qs}^{e*} \tag{9}$$

$$i_{qs}^{e*} = \frac{2}{3} P_{req} \frac{L_r}{L_m{}^2 w_r i_{ds}^{e*ss}} \tag{10}$$

Here in these equations, P_{req} is the estimated average active power required from the flywheel induction machine, T_e is the generated electrical torque of the flywheel induction machine, ω_r is the rotor electrical angular frequency, L_m is the per phase magnetizing inductance, L_r is the per phase total stator referred rotor inductance, i_{ds}^{e*ss} is the steady state stator flux component current command in synchronous reference frame, and i_{qs}^{e*} is the stator torque component current command in synchronous reference frame.

Before the estimated torque component current command is applied to the flywheel induction machine, a minor contribution from the PI peak link voltage regulator is added to the estimation to prevent excessive peak link voltage variations as a result of instantaneous mismatches between the incoming and outgoing average active powers, estimation errors, and parameter variations. The system is sensitive to the rotor time constant to a certain extent since this constant is determined at the beginning and assumed as such throughout the operation. The only regulation that takes measure against the variations of the parameters is the above mentioned PI peak link voltage regulator. The system performance, however, could be improved by very careful design of a parameter insensisitve system.

III.C. Software Simulation Results

The load machine and flywheel inertia were chosen to be 0.07 and 0.2 kgm^2 respectively and the simulation time interval to be 6.5 sec. A 2.5 kW average power was assumed to be delivered to the system by the constant power source. The initial speed of the flywheel was assumed to be 4000 rpm. A parallel equivalent loss resistor of 0.03 ? for the resonant tank circuit was assumed.

Figure 4 shows basically what happens to the speed of the flywheel and the peak link voltage during the flywheel mode of operation under the specified operating conditions. Here the load machine operates in four different quadrants of operation. The figure shows the start of flywheel mode of operation at time t=0.35 sec with the start of torque component current command application to the flywheel machine. Prior to the flywheel mode of operation, the necessary power balance in

the system is maintained by the initial charging circuit. During the flywheel mode of operation

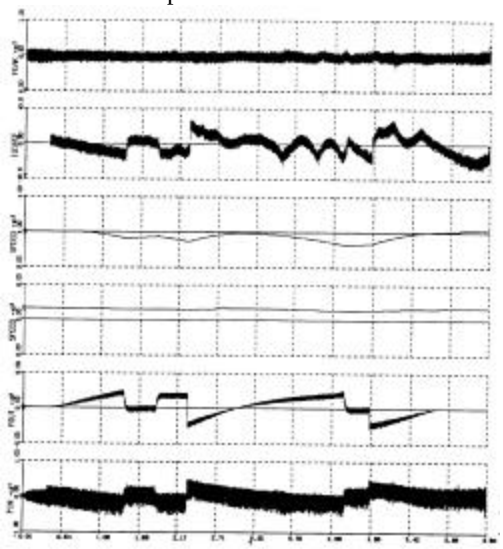

Fig. 4. Dynamic Response of the Flywheel to Varying Power Demands of the Load and Losses with the Operating Conditions Stated in Section II.C. From the Top: **PEAK**: HF Peak Link Voltage [0, 500, 1000] V. **IQSREF**: Estimated Torque Component Current Command for the Flywheel [-40, 0, +40] A. **SPEED**: Speed of the Flywheel [3500, 4000, 4500] rpm. **SPEED**: Speed of the Flywheel [0, 3000, 6000] rpm. **POUT**: Average Real Load Machine Power [-5000, 0, 5000] W. **PIN**: Average Active Power of the Flywheel Machine [-10000, 0, 10000] W. Time/div: 542 ms.

the load machine has a very dynamic and varying power demand from the system as can be observed from the fifth trace from the top. The flywheel machine therefore should be given a proper torque component current command to maintain the entire power balance in the system and achieve a proper peak link voltage. The second trace from the top shows such torque component current command reference for the flywheel machine. The first trace shows a well regulated peak link voltage throughout the entire operation. The third and fourth traces from the top show the speed of the flywheel in various speed ranges. The third trace, being the more precise, clearly shows that the speed of the flywheel is initially 4000 rpm and later on it goes through some variations depending on the load levelling requirements.

Figure 5 shows different traces of the same operation in Fig. 4., namely, flywheel and load machine torque component current commands, line current references and actual line currents. Both machines are given full rated flux commands and therefore fully excited during the flywheel mode of operation. Therefore, whenever there is a change in the torque component current command there is also a corresponding change in the line currents of the related machine. Since the flywheel machine is operating at around 200 Hz while the load machine is operating at less than 60 Hz the load side machine line currents are easier to follow with respect to flywheel machine line currents. Load machine line currents also show a phase reversal near the middle of the trace because of the speed reversal and consequent change in the quadrant of operation.

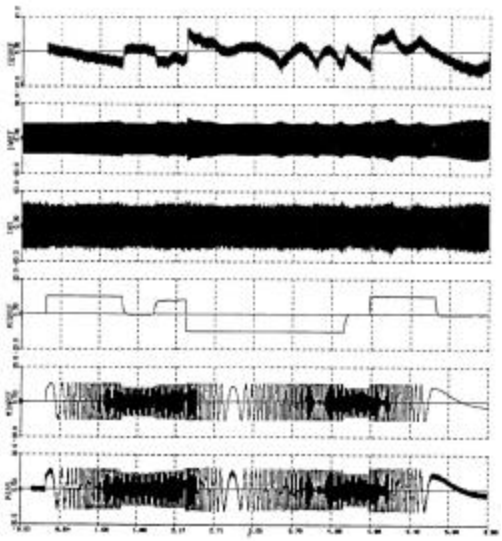

Fig. 5. Response of the Machine Line Currents to their Varying Torque Commands with Rated Excitation and Same Operating Conditions of Fig. 4. From the Top Respectively: **IQSREF:** Estimated Torque Component Current Command for the Flywheel [-40, 0, +40] A. **IAREF:** Flywheel Machine Phase-A Line Current Reference [-60, 0, +60] A. **IAS:** Flywheel Machine Phase-A Line Current[-60, 0, +60] A. **MIQREF:** Torque Component Current Command of the Load Machine[-20, 0, +20] A. **MIAREF:** Load Machine Phase-A Line Current Reference [-30, 0, +30] A. **MIAS:** Load Machine Phase-A Line Current [-30, 0, +30] A. Time/div: 542 msec.

III.D. Limits of the Flywheel Machine

Figure 6 is intended to show the limits of the flywheel machine by intentionally setting certain initial conditions and flywheel machine inertia to critical values. Here, a bad machine inertia of 0.01 kgm^2, a constant source power delivery of 3.0 kW, a 0.1 kgm^2 flywheel inertia, 3000 rpm initial flywheel speed, and a 2.5 sec simulation time interval is assumed. As the traces shown in Fig. 6 reveal, reducing the initial flywheel speed and the inertia, and the constant power delivery to the system while increasing the applied load level results in a higher amplitude of torque component current commands for the flywheel. Furthermore, when the load machine enters the second quadrant of operation which corresponds to the regenerating region, the torque component current command for the flywheel reaches its limit value and does not become sufficiently large to absorb the extra power pumped to the link. As a result, the peak link voltage goes out of control and continues to increase because of this unabsorbed extra power dumped onto the link until the regenerated load-machine power reduces in amplitude to a value that flywheel can absorb or handle with its current speed and inertia. This figure thus clearly conveys messages as to what should be the minimum speed and inertia of the flywheel, and how much power can be extracted or absorbed and how long.

IV. EXPERIMENTAL REALIZATION

A power circuit and control block diagram of the experimental system is shown in Fig. 7. One of the existing two converter bridges in hardware is used for the initial charging circuit and constant power source, and the other is used for the flywheel induction machine interface.

The battery and its source side converter of the software simulated system is replaced by a three phase (3Ø), 60 Hz utility source and an associated 3Ø-PDM converter. The constant power source characteristic of the battery is conveniently modelled by tight control of the source side converter power. A 3Ø, 300 Hz, 10 Hp induction machine with a dc dynamometer and two flywheel inertia discs coupled to the same shaft is used as flywheel for the system. This machine is connected to the ac link via another 3Ø-PDM converter.

The induction machine load of the software simulated system is replaced by manually switched resistor blocks across the ac link in the hardware prototype. Therefore, the need for a third converter interface to the link is eliminated. Turning on and off different levels of active power by connecting/disconnecting power resistors across the link results in varying power demands from the system and the power balance in the ac link is maintained by the flywheel machine. In other words, when extra power is pumped into the link, the flywheel absorbs the extra power and speeds up, and when load and losses demand more power than the system can deliver, the flywheel delivers that required power to the

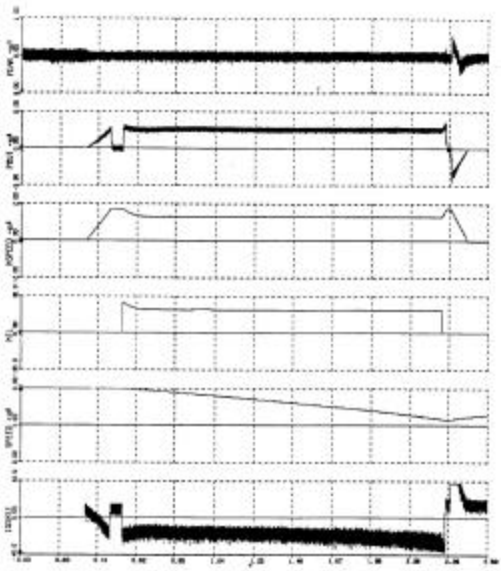

Fig. 6. Software Simulation Results Showing the Limits of the Flywheel Machine with Intentionally Set Initial Conditions and Small Flywheel Inertia. From the Top Respectively: **PEAK:** HF Peak Link Voltage [0, 500, 1000] V. **POUT:** Average Real Load Machine Power [-5000, 0, 5000] W. **MSPEED**: Speed of the Load Machine [-2000, 0, 2000] rpm. **MTL**: Load Torque Applied to the Load Machine [-30, 0, +30] Nm. **SPEED**: Speed of the Flywheel [0, 1500, 3000] rpm. **IQSREF**: Estimated Torque Component Current Command for the Flywheel [-40, 0, +40] A. Time/div: 208 msec.

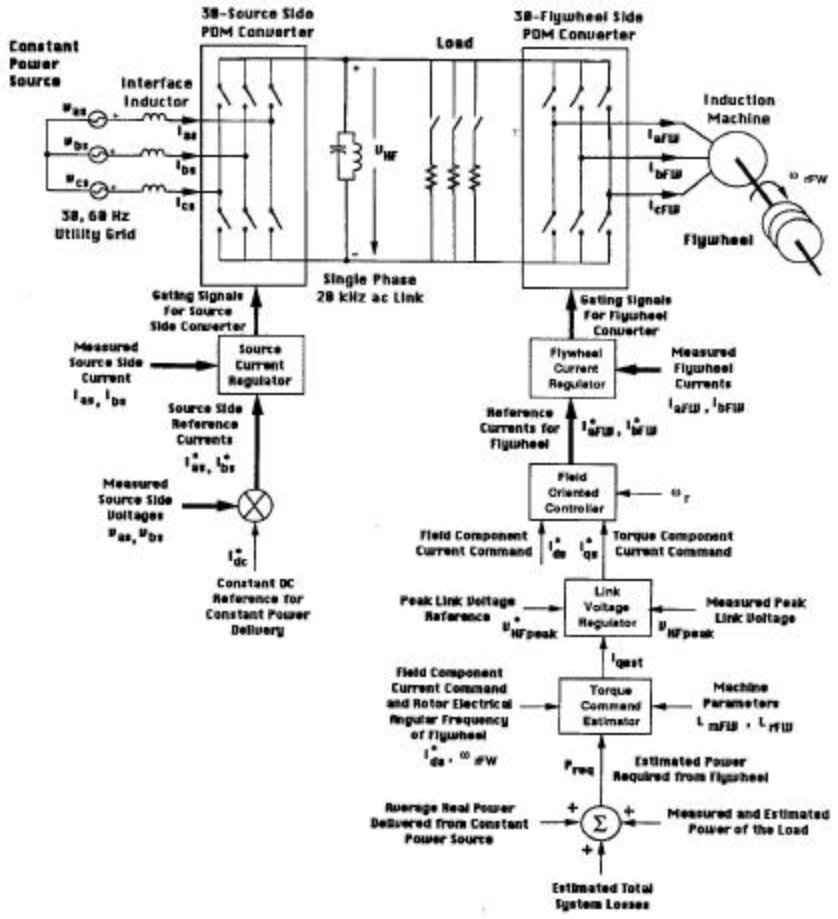

Fig. 7. Power and Control Block Diagram of the Hardware Prototype Flywheel Energy Storage and Load Leveling System

link and speeds down. The experimental results of this type of operation is presented in this section.

IV.A. Specifications of the Source, Load and the Flywheel

The 3Ø, 60Hz utility grid operating via 3Ø-PDM converter from 20kHz ac link is used as constant power source for the system. The line to line voltage of the source is set to $150V_{rms}$. A sinusoidal current reference having a $13.6A_{peak}$ value is used. These given specifications imply a constant power delivery of about 2.5kW from the source to the system. The nameplate ratings and per phase equivalent circuit parameters of the induction machine used in the experiment as flywheel are given in Appendix 1. Several 1kW power resistors operating from $500V_{peak}$ ac link are used as load units. These 1-kW load units are connected/disconnected across the 20kHz ac link using manual switches.

IV.B. Principle of Operation of the Experimental System

In order to energize the system, the reference peak link voltage is established across the parallel resonant 20kHz ac link. The induction machine is excited and brought up to some sufficient speed before it is operated as a flywheel. Since no extra excitation capacitors is used, the excitation of the induction machine is achieved via operation of the associated 3Ø-PDM converter from the 20kHz ac link.

As is apparent, this initial starting process can not be achieved by simply utilizing a constant power delivery/flywheel mode of operation. Therefore, initially, the 3Ø, 60 Hz utility grid is not used as a constant power source rather it is used as a power balancing source in the process of establishing the reference peak link voltage, exciting the flywheel machine and bringing it to its desired speed in speed regulation mode before it is used as flywheel. After these initial requirements are met, a manual controller switch is used to initiate the flywheel mode of operation along with 3Ø, 60 Hz utility grid control to perform a constant power delivery mode of operation. After the new setting, the induction machine is operated so as to balance the power in the link and maintain a proper link voltage by a proper estimation of the torque component current command of the flywheel induction machine as described in the preceding section. Power consumption of the load resistors are measured and included in the required power and torque command estimation for the flywheel machine.

The control of the average active power balance in the link is achieved in the same manner as described in Section III.A. The only changes concern the specifications of the

source and the load and the manner for determining how much power the load is drawing.

IV.C. Experimental Operation Results

Before the flywheel mode of operation is set, the induction machine used as flywheel is excited with rated flux command and the machine is brought up to a speed of approximately 2,700rpm. In the flywheel mode of operation 2.5kW constant power is delivered from the 3Ø, 60Hz utility source to the system via associated 3Ø-PDM converter. The pictures presented here are taken for a flywheel mode of operation persisting longer than 10 sec which clearly demonstrates the feasibility of operation of the overall system.

Figure 8 shows the experimental performance of the flywheel mode of operation of the system under load variations. Note that the peak of the 20kHz high frequency link voltage is well regulated during the entire mode of operation. The first trace from the top shows the load current. Initially, until the first level of load is applied there is a small positive torque component current during which the flywheel machine operates as a motor and absorbs a corresponding power.

When the first level of load, approximately 1-kW, is applied, a negative 10A torque component current command is generated by the flywheel motor controller to meet this load demand in which the flywheel machine operates as a generator and delivers a corresponding power. In the motoring mode flywheel tends to speed up and in the generating mode it tends to speed down. As the level of power absorbed/delivered increases, the process of speeding up/down gets faster. In the generating mode of operation, the torque component current command has a tendency to increase in amplitude for the same power delivery level to meet the same active power demand of the system as the flywheel speed reduces.

When another 1-kW load is added to the previous load the controller immediately responds to the change by increasing the torque component current command from around 10A levels to 30A levels depending of course on the speed of the flywheel at that instant. Since more energy is extracted from the flywheel during this time, the speed of the flywheel reduces more rapidly.

When one of the 1-kW load is removed from the system, the controller responds again but not so fast as when the load is applied. Nonetheless, the peak link voltage is still regulated within an acceptable range. The reason for the slow response

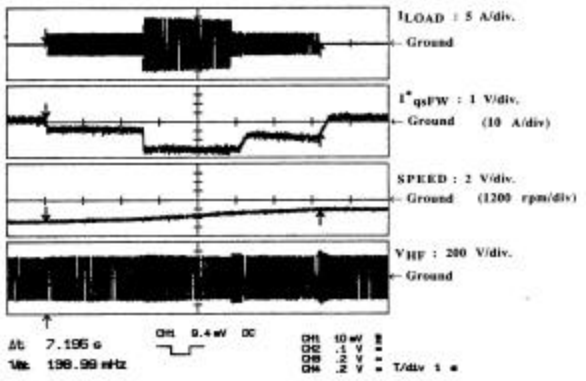

Fig. 8. Performance of Operation of the Experimental Flywheel Load Levelling System under 2.5kW Constant Power Delivery and Two Different Level of Load Application and Removal. $\boldsymbol{I_{LOAD}}$**:** Load Current, 5A/div. $\boldsymbol{I^*_{qsFW}}$: Torque Component Current Command of the Flywheel Induction Machine, 10A/div. **Speed :** Speed of the Flywheel, 1200 rpm/div. $\mathbf{V_{HF\,Link}}$ **:** 20kHz High Frequency AC Link Voltage, 200V/div. Time/div: 1 s.

of the controller is probably due to the time constant of the peak detection circuits of the measurement systems. It is interesting to note that the torque component current command increases to about 15A levels even though the remaining load is 1-kW compared to the 10A levels with 1-kW load at the beginning of operation. This result is due to the reduced speed of the flywheel as mentioned earlier.

When all the remaining load is removed from the system, the controller generates a positive torque command with a small amplitude and the flywheel machine tends to absorb power and increase its speed in this mode. It is difficult to observe the details of the load current and the 20 kHz lnk voltage in this trace because of the very low frequency of the data taken.

The terminal quantities of the flywheel machine, namely the line current and line to line voltage, are presented in Figure 9 for a similar operation and different time interval. There is a line current flowing and a very little torque command exists during the no load condition due to the excitation current of the flywheel machine. Whenever the torque command level changes a corresponding change in the line current is observed. This figure clearly shows how the flywheel line to line voltage is synthesized from the portions of the 20 kHz parallel resonant ac link and indicates how the line current regulation of the flywheel machine is achieved depending on the torque command applied.

It is possible to increase the operating time interval of the flywheel mode by increasing the initial speed and inertia of the flywheel. If the lab environment would allow higher speed of operations, the induction machine used as flywheel whose nameplate ratings and equivalent circuit parameters are given in Appendix-1 would allow 6000 rpm operation at rated flux and 18000 rpm operation in reduced flux region.

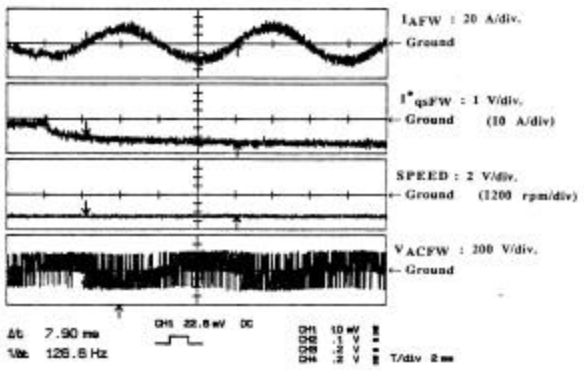

Fig. 9. Performance of Operation of the Flywheel Machine Concerning Its Electrical Quantities. $\mathbf{I_{AFW}}$**:** Phase-A Flywheel Induction Machine Current, 20A/div. $\mathbf{I^*_{qsFW}}$: Torque Component Current Command of the Flywheel Induction Machine, 10A/div. **Speed :** Speed of the Flywheel, 1200 rpm/div. $\mathbf{V_{ACFW}}$ **:** Phase-AC Line to Line Voltage of the Flywheel, 200V/div. Time/div: 1 ms.

IV. CONCLUSIONS

In this study, the feasibility of induction machine based flywheel load levelling system fed from a 20kHz ac link and Pulse Density Modulated (PDM) converter has been demonstrated both in software and hardware. The feasibility of maintaining a relatively constant ac peak link voltage by rapidly extracting or absorbing excess link power from/to a flywheel induction machine connected to the link was demonstrated as well. A detailed evaluation of the control requirements for such a control strategy has been developed, implemented and demonstrated.

An important contribution of this work has been to demonstrate the application of 20kHz ac link and PDM converter technology to FES systems. In particular, aerospace applications are well suited to benefit from the advantages provided by this technology.

APPENDIX 1

3-Phase (3Ø), 10Hp, 230V, 32A, 300Hz, 6-poles
6000rpm @ No Load, 5957rpm @ Rated Torque
?-Connected Stator Winding, Squirrel Cage Rotor
Designed to Operate at 900Hz (18,000rpm) with Field Weakening,

r_{1dc} =0.195?
r_2' =0.10482?
r_M =240? @ 300Hz and 40.411? @ 60Hz
$L_{1l} = L_{2l}'$=0.6796mH at 60Hz
L_M =11.149mH at 300Hz and 10.888mH at 60Hz
S_R =0.0072 @ $230V_{ll}$/300Hz and Rated Torque
S_R =0.0358 @ $46V_{ll}$/60Hz and Rated Torque

APPENDIX 2

3-Phase (3Ø), 10Hp, 230V/460V, 24.2A/12.1A, 60-Hz, 4-poles, 1800rpm @ No Load, 1750 rpm @ Rated Torque
Star-Connected Stator Winding, Squirrel Cage Rotor
r_{1dc} =0.1844?
r_2' =0.2009?
r_M =197.89? @ 60Hz and 230 V
r_M =113.98? @ 60Hz and 115 V
r_M =33.007? @ 60Hz and 50 V
$L_{1l} = L_{2l}'$=1.4345mH with Measurement at 60Hz
L_M =37.577mH at 60Hz and 230V
L_M =38.598mH at 60Hz and 115V
L_M =35.448mH at 60Hz and 50V
S_R =0.02777 @ $230V_{ll}$/60Hz and Rated Torque

V. REFERENCES

[1] Van Zyl A.; Spee , R.; *"Short Term Energy Storage for ASD Ride-Through"*, IEEE Industry Applications Conference, 1998. The 33rd IAS Annual Meeting Conference Records, Vol. 2, pp. 1162-1167.

[2] Christopher, D.A.; Beach, R.; *"Flywheel Technology Development Program for Aerospace Applications"*, IEEE Aerospace and Electronics Systems Magazine, June 1998, pp. 9-14.

[3] Christopher, D.A.; Donet, C.; *"Flywheel Technology and Potential Benefitsfor Aerospace Applications"*, IEEE 1998 Aerospace Conference, Conference Records, Vol. 1, pp.159-166.

[4] Kirk. J.A.; Walsh, G.C.; Hromada, L.P.; Zmood, R.P.; Sullivan, G.E.; *"The Open Core Composite Flywheel"*, Proceedings of the 32nd Intersociety Energy Conversion Engineering Conference, 1997. IECEC-97, Vol. 3, pp.1748-1753.

[5] Edwards, J.; Aldrich, J.W.;Christopher, D.A.; Beach, R.F.; Barton. J.R.; *"Flight Test Demonstration of a Flywheel Energy Storage System on the International Space Station"*, Procedings of the IEEE 1997 NationalAerospace and Electronics Conference, NAECON-97, Vol. 2, pp. 617-621.

[6] Christopher, D.A.; Beach, R.F.; Barton. J.R.; *"Flywheel Energy Storage System Test on the International Space Station"*, Procedings of the 32nd Intersociety Energy Conversion Engineering Conference, IECEC-97, Vol. 3, pp. 1762-1766.

[7] Robinson, W.; Hanks, J.; Gisler, O.; Spina, L.; Ginter, D.S.; *"Spacecraft Energy Storage Systems"*, Procedings of the IEEE 1997 NationalAerospace and Electronics Conference, NAECON-97, Vol. 2, pp. 609-616.

[8] Pieronek, T.J.; Decker, D.K.; Spector, V.A.; *"Spacecraft Flywheel Systems-Benefits, and Issues"*, Procedings of the IEEE 1997 NationalAerospace and Electronics Conference, NAECON-97, Vol. 2, pp. 589-593.

[9] Beaman, B.G.; Rao, G.M.; *"Hybrid Battery and Flywheel Energy Storage System for LEO Spacecraft"*, The Thirteenth Annual Battery Conference on Applications and Advances, 1998. Conference Records, pp. 113-116.

[10] Chu, A.; Nowicki, E. P.; Chen, T.; *"Design of a Robust Speed Controller for a Compressor Driven by a Field Oriented Controlled Induction Motor"*, IEEE Canadian Conference on Electrical and Computer Engineering, 1998, Conference Records, Vol. 2, pp. 481-484.

[11] Rutberg, P.; Ivanov, V.; Kashkarsky, E.; Kustov, N.; Rovinsky, P.; *"Electrotransmission of Alternating Current with Flywheel for Wheel Transport Facility"*, MELECON'98, 9th Mediterranian Electrotechnical Conference, 1998, Conference Records, Vol. 2, pp. 1152-1156.

[12] Szabodos, B.; Schaible, U.; *"Peak Power Bi-Directional Transfer from High Speed Flywheel to Electrical Regulated Bus Voltage System: A Practical Proposal for Vehicular Technology"*, IEEE Transactions on Energy Conversion, March 1998, Vol. 13, Issue 1, pp. 34-41.

[13] Acarnely, P.P.; Mecrow, B.C.; Burdess, J.S.; Fawcett, J.N.; Kelly, J.G.; Dickinson, P.G.; *"Design Principles for a Flywheel Energy Store for Road Vehicles"*, IEEE Transactions on Industry Applications, Nov.-Dec. 1996, Vol. 32, Issue 6, pp. 1402-1408.

[14] Weissbach, R.S.; Karady, G.G.; Farmer, R.G; *"Dynamic Voltage Compensation on Distribution Feeders Using Flywheel Energy Storage"*, IEEE Transactions on Power Delivery, April 1999, Vol. 14, Issue 2, pp. 465-471.
[15] Uemura, S.; Nomura, S.; Shimada, R.; *"Stabilization of Electric Power System Using the Variable Speed Flywheel Generator"*, Proceedings of the Power Conversion Conference, Nagaoka 1997, Vol.1, pp. 215-218.
[16] Nishio, T.; Minoguti, K; Uno, S.; Futami, M.; Hombu, M; Ichinose, M.; Maoka, A.; *"Continuous Operation Control During Electric Power Network Faults in an Adjustable Speed Generation System with a Flywheel Excited by a DC Link Converter"*, Proceedings of the Power Conversion Conference, Nagaoka 1997, Vol.1, pp. 209-214.
[17] Schoenung, S.M.; Burns, C.; *"Utility Energy Storage Applications Studies"*, IEEE Transactions on Energy Conversion, Sep. 1996, Vol. 11, Issue 3, pp. 658-665.
[18] Bornemann, H.J.; Sander, M.; *"Conceptual System Design of a 5 MWh/100MW Superconducting Flywheel Energy Storage Plant for PowerUtility Applications"*, IEEE Transactions on Aplied Superconductivity, June 1997, Vol. 7, Issue 2, Part-1, pp. 398-401.
[19] Sul, S.K.; Alan, I.; Lipo T.A.; *"Performance Testing of a High Frequency Link Converter for Space Station Power Distribution System"*, 1989 Intersociety Energy Conversion Engineering Conference, Washington DC, August 1989, Vol. 1, Aerospace Power Systems and Power Conditioning, pp. 617-624.
[20] Lipo, T.A.; Alan, I.; *"System and Component Design and Test of a 10 HP, 18,000 RPM AC Dynamometer Utilizing a High Frequency AC Voltage Link"*, Final Report, Contract No. NAG3-940, June 1991.
[21] Alan, I.; *"A Completely Isolated 3-Phase to 3-Phase Induction Motor/Induction Generator Power Conversion System"*, Ph.D. Thesis, December 1993.
[22] Alan, I.; Lipo, T.A.; *"Control of Polyphase Induction Generator/Induction Motor Power Conversion System Completely Isolated from the Utlity"*, IEEE Transactions on Industry Applications, Vol. 30, No.3, May-June 1994, pp. 636-647.
[23] Alan, I.; Lipo, T.A.; *"Feasibility Study of a Battery Started Induction Generator Maintained 3-Phase/400Hz Voltage Regulated Bus Utilizing High Frequency AC Link"*, Final Report, Contract No. NAG3-1447, May 1995.
[24] Novotny D.W.; Lipo, T.A.; *"Vector Control and Dynamics of AC Drives"*, NewYork: Oxford Univ. Press, 1996.
[25] Divan D.M.; Lorentz R.D.; Lipo T.A.; Novotny D.W.; *"Field Orientation and High Performance Motion Control", UW-Madison, WEMPEC, Summary of Publications 1981-1988.*
[26] Sood P.K.; Lipo T.A.; *"Power Conversion Distribution System Using a Resonant High Frequency AC Link"*, IEEE Transactions on Industry Applications, March-April 1988, Vol. 24, pp. 288-300.
[27] Divan D.M.; Lasseter R.H.; Lorentz R.D.; Lipo T.A.; Novotny D.W.; *"Soft Switching Converters: Topologies, Design and Control", UW-Madison, WEMPEC, Summary of Publications 1986-1990.*

Irfan Alan (S'91-M'94) was born in Istanbul, Turkey. He received the B.E.E. and M.S.E.E. degrees from Istanbul Technical University (ITU), in 1983 and 1986, and the Ph.D. degree in E.E. from the University of Wiscconsin-Madison, in 1993.

He was appointed a Research Assistant during his M.S. studies at ITU. In 1986 he was awarded a loan scholarship by the Turkish Ministry of Education to pursue a Ph.D. degree abroad. During most of his Ph.D. studies he has been a research assistant at UW-Madison, working on various NASA projetcs. He worked as a research associate at UW-Madison in another NASA project during his post doctorate studies. He has submitted a total of four contractor reports to NASA. He is currently an Associate Professor teaching various undergrad and grad level Electrical-Electronics and in particular Electrical Machines and Power Electronics courses at the Department of Electrical and Electronics Engineering of Ege University in Izmir, Turkey. His research interests are in solid state power conversion systems and ac machine drives in general, and resonant and matrix power converters and drives in particular.

Thomas A. Lipo (M'64-SM'71-F'82) was born in Milwaukee, WI. He received the B.E.E. and M.S.E.E. degrees from Marquette University Milwaukee, WI. in 1962 and 1964, and the Ph.D. degree in electrical engineering from the University of Wisconsin in 1968.

From 1969 to 1979, he was an Electrical Engineer in the Power Electronics Laboratory of Cooperate Research and Development of the General Electric Company, Schenectady, NY.

He became Professor of Electrical Engineering at Purdue University, West Lafayette, IN, in 1979, and in 1981 he joined the University of Wisconsin, Madison, in the same capacity, where he is presently the W. W: Grainger Professor for Power Electronics and Electrical Machines.

Dr. Lipo received the Outstanding Achievement Award from the IEEE Industry Applications Society, William E. Newell Award of the IEEE Power Electronics, and the 1995 Nicola Tesla IEEE Field Award from the Power Engineering Society for his work. He has served IEEE in various capacities, including President of Industrial Applications Society.